Overview of supplemental materials

Table S1: AF model scores
Table S2: Mass spectrometry data
Supplemental dataset 1:alphafold models pdb files.

Figure S1: AF score plots and comparison to cryo-EM models.
Figure S2: Validation of novel binders and AF models of distinct binding mechanisms.
Figure S3: CDCA4 data.
Figure S4: IER2 data.
Figure S5: RBM7 data.
Figure S6: PME1 data.
Figure S7: EYA3 data.
Figure S8: AMOTL2 data.
Figure S9: Zds1 data.
Figure S10: E4ORF4 data.
Figure S11: Conservation of SERTA domains.
Figure S12: Volcano plots of MS data.
Figure S13: B55 mutant IPs with CDCA4.
Figure S14: Protein MPNN scores in relation to binding.
Figure S15: SPR data for PME1, Arpp19 and RBM7.
Figure S16: Western blots relating to RBM7 biology and RBM7 SPR data.

A

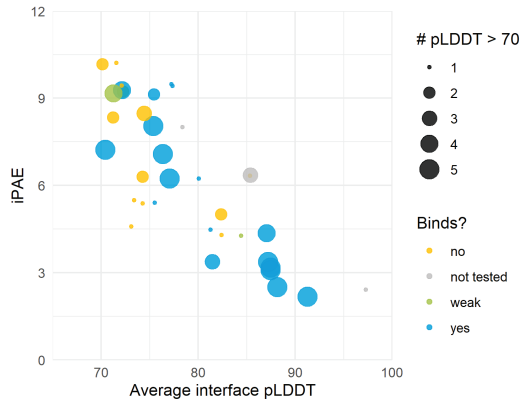

B

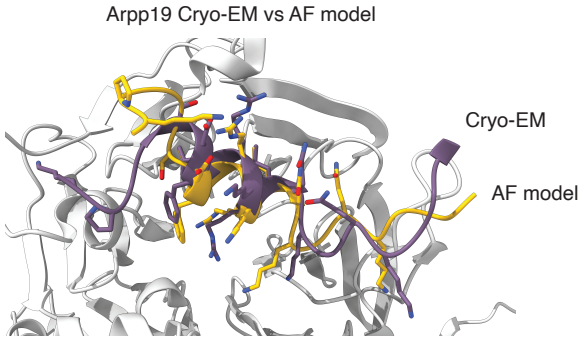

C

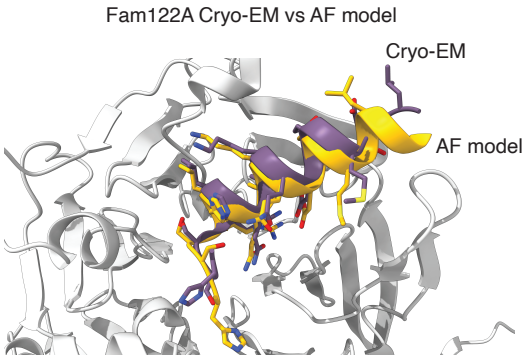

Supplemental Figure S1.
A) Plot showing iPAE and pLDDT score for the 36 models and whether they were binding to PP2A-B55 in immunoprecipitation experiments. The size of the dot indicates number of models with a pLDDT above 70. **B)** Overlay of the Arpp19 cryo-EM structure (PDB: 8TTB) with the AF model focusing on the helix binding B55. **C)** Overlay of the FAM122A cryo-EM structure (PDB: 8SO0) with the AF model focusing on the helix binding B55.

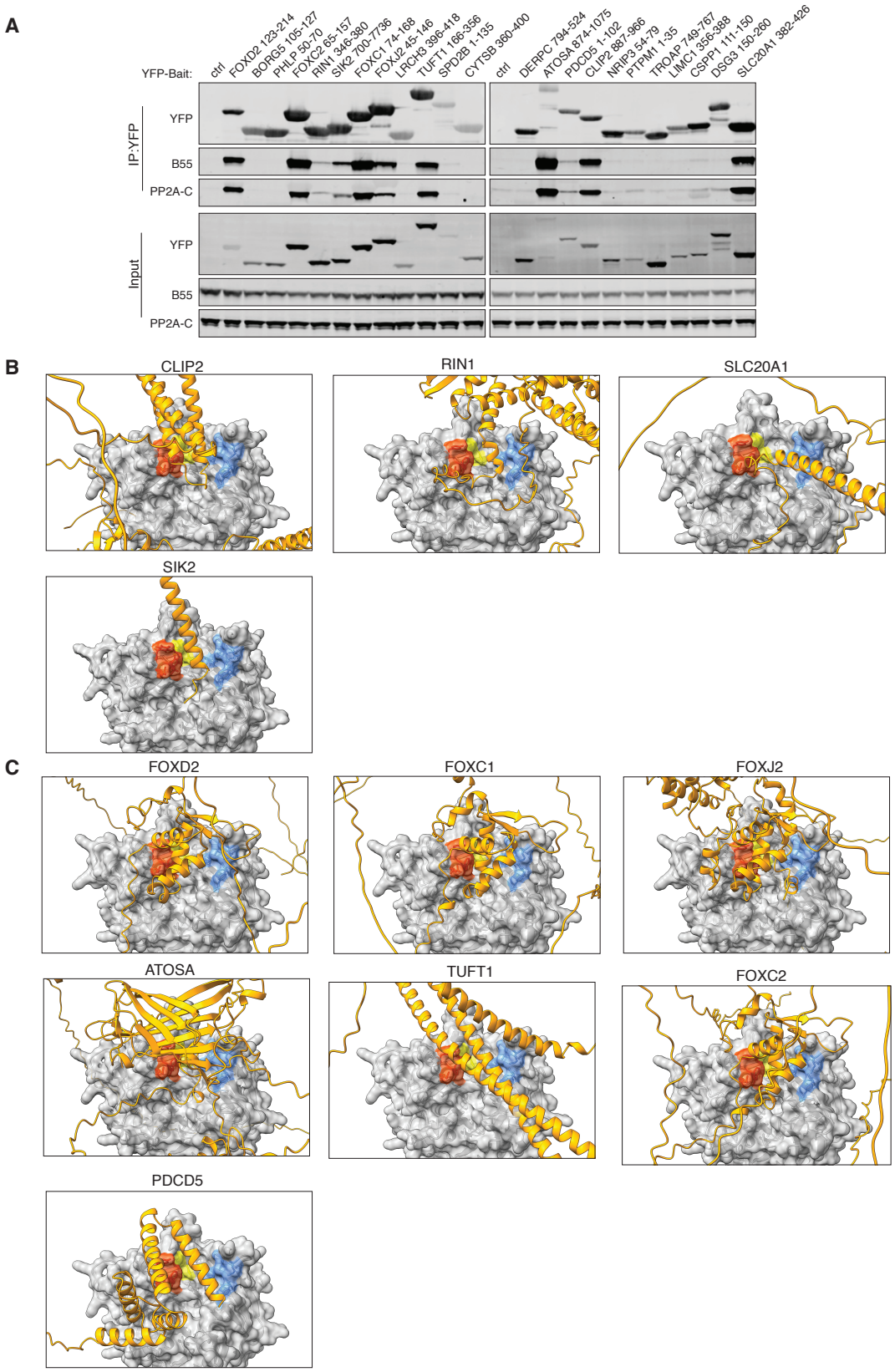

Supplemental Figure S2

A) The indicated YFP tagged protein fragments were expressed in HeLa cells and following immunoprecipitation they were probed for binding to PP2A-B55 by western blot. **B)** AF models of the indicated proteins binding to PP2A-B55 in a common manner. **C)** AF models of the indicated proteins binding to PP2A-B55 in a distinct manner.

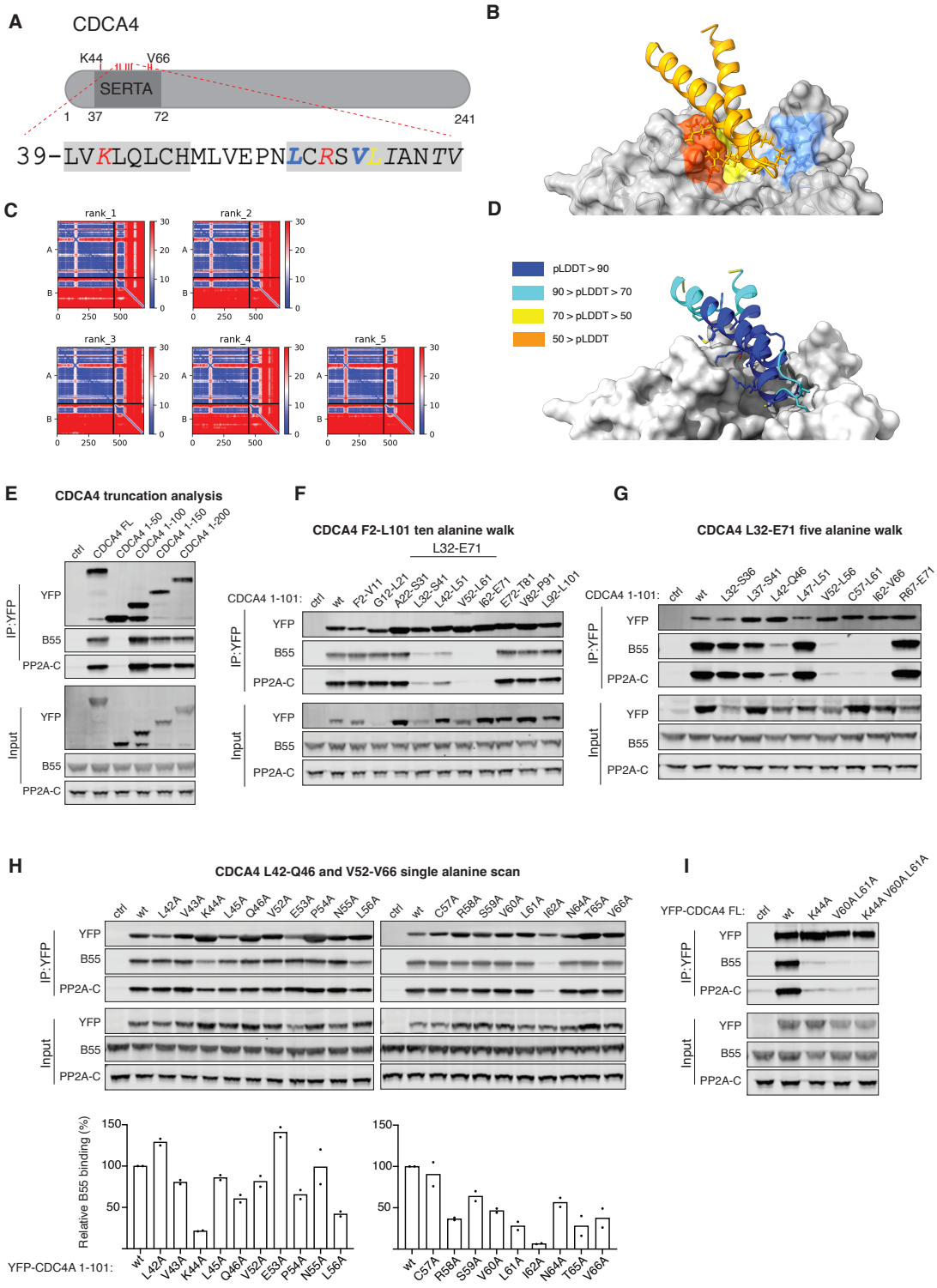

Supplemental Figure S3

A) Schematic of CDCA4 and sequence binding PP2A-B55. **B**) AF model of CDCA4 bound to B55. **C**) Prediction aligned error (PAE) score for the 5 models. **D**) pLDDT score mapped onto model. **E-I**) The indicated YFP tagged protein fragments were expressed in HeLa cells and following immunoprecipitation they were probed for binding to PP2A-B55 by western blot. In H) the quantification of two experiments is shown with binding normalized to wild type protein.

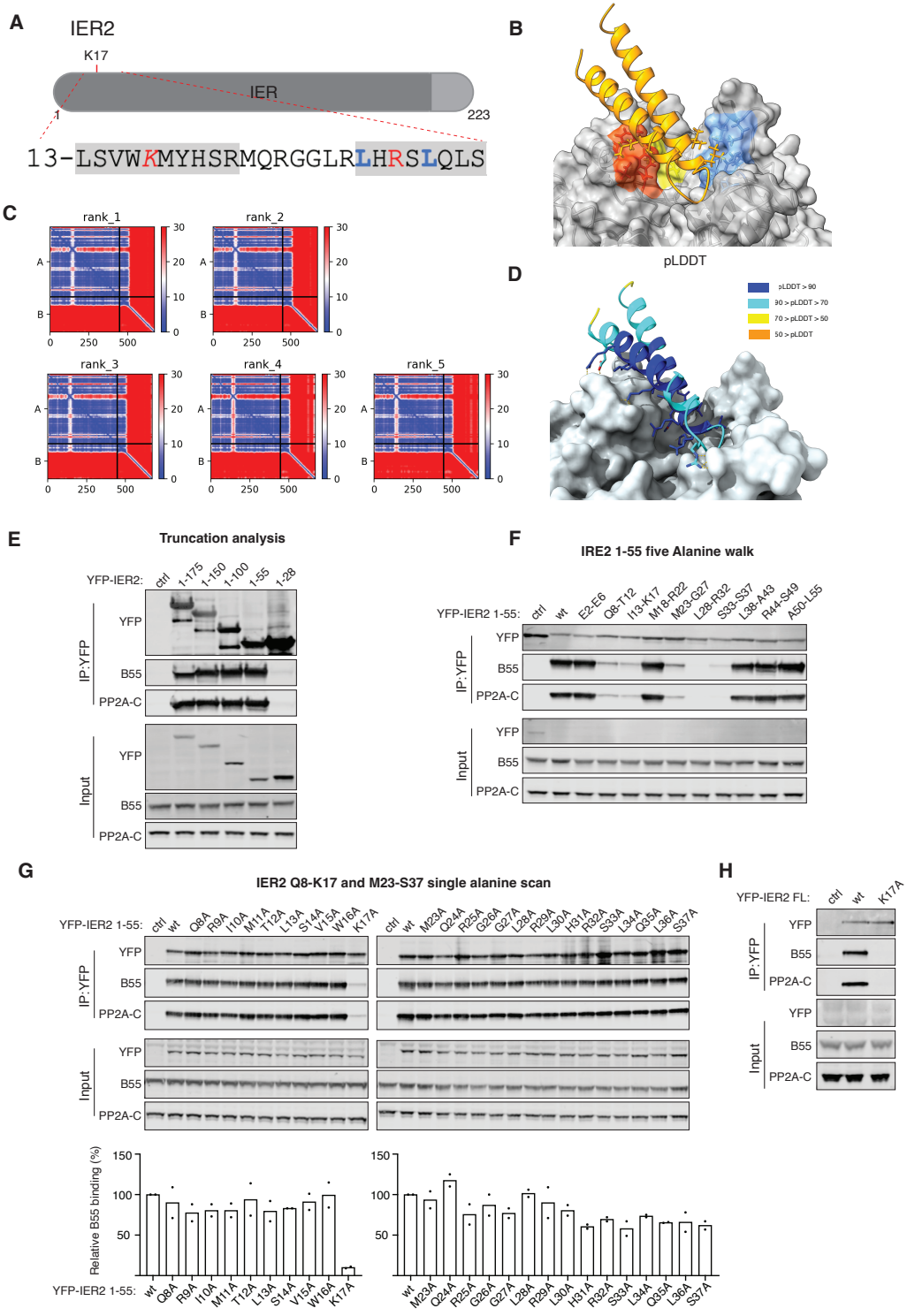

Supplemental Figure S4

A) Schematic of IER2 and sequence binding PP2A-B55. **B**) AF model of IER2 bound to B55. **C**) Prediction aligned error (PAE) score for the 5 models. **D**) pLDDT score mapped onto model. **E-H**) The indicated YFP tagged protein fragments were expressed in HeLa cells and following immunoprecipitation they were probed for binding to PP2A-B55 by western blot.

In G) the quantification of two experiments is shown with binding normalized to wild type protein.

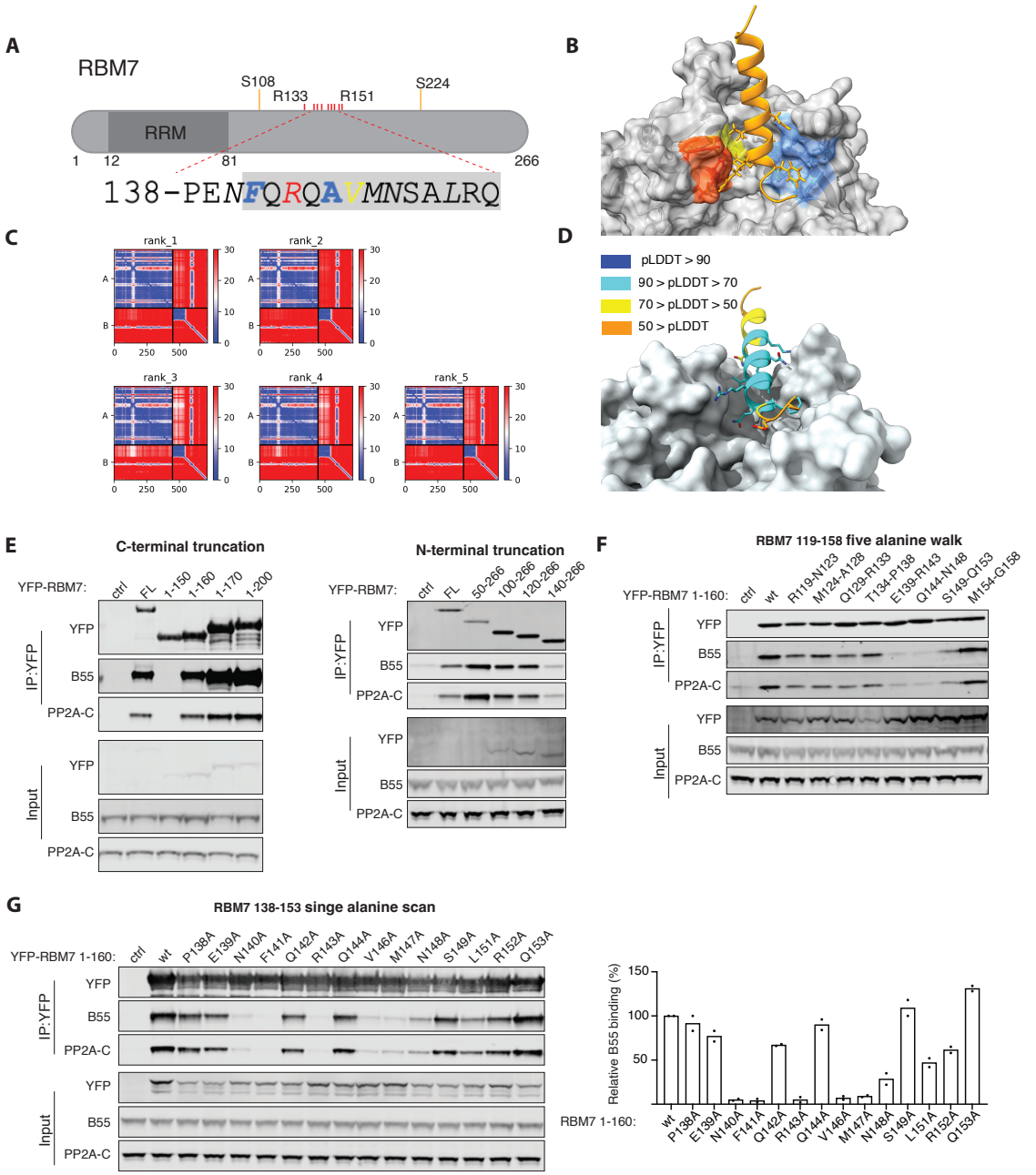

Supplemental Figure S5

A) Schematic of RBM7 and sequence binding PP2A-B55. Phosphorylation sites with higher occupancy in RBM7 R143A indicated. **B**) AF model of RBM7 bound to B55. **C**) Prediction aligned error (PAE) score for the 5 models. **D**) pLDDT score mapped onto model. **E-H**) The indicated YFP tagged protein fragments were expressed in HeLa cells and following immunoprecipitation they were probed for binding to PP2A-B55 by western blot. In H) the quantification of two experiments is shown with binding normalized to wild type protein.

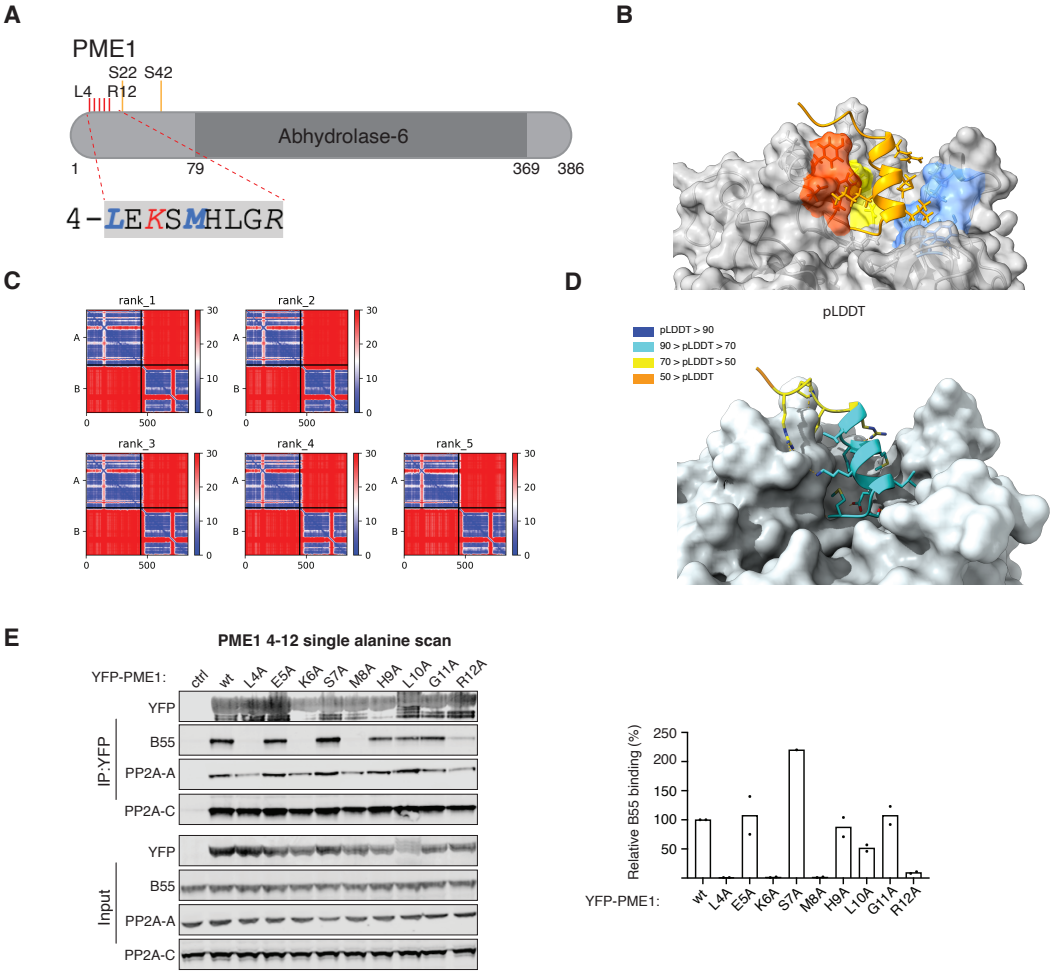

Supplemental Figure S6

A) Schematic of PME1 and sequence binding PP2A-B55. Phosphorylation sites with higher occupancy in PME1 L4A indicated. **B**) AF model of PME1 binding helix bound to B55. **C**) Prediction aligned error (PAE) score for the 5 models. **D**) pLDDT score mapped onto model. **E**) The indicated YFP tagged proteins were expressed in HeLa cells and following immunoprecipitation they were probed for binding to PP2A-B55 by western blot. The quantification of two experiments is shown with binding normalized to wild type protein.

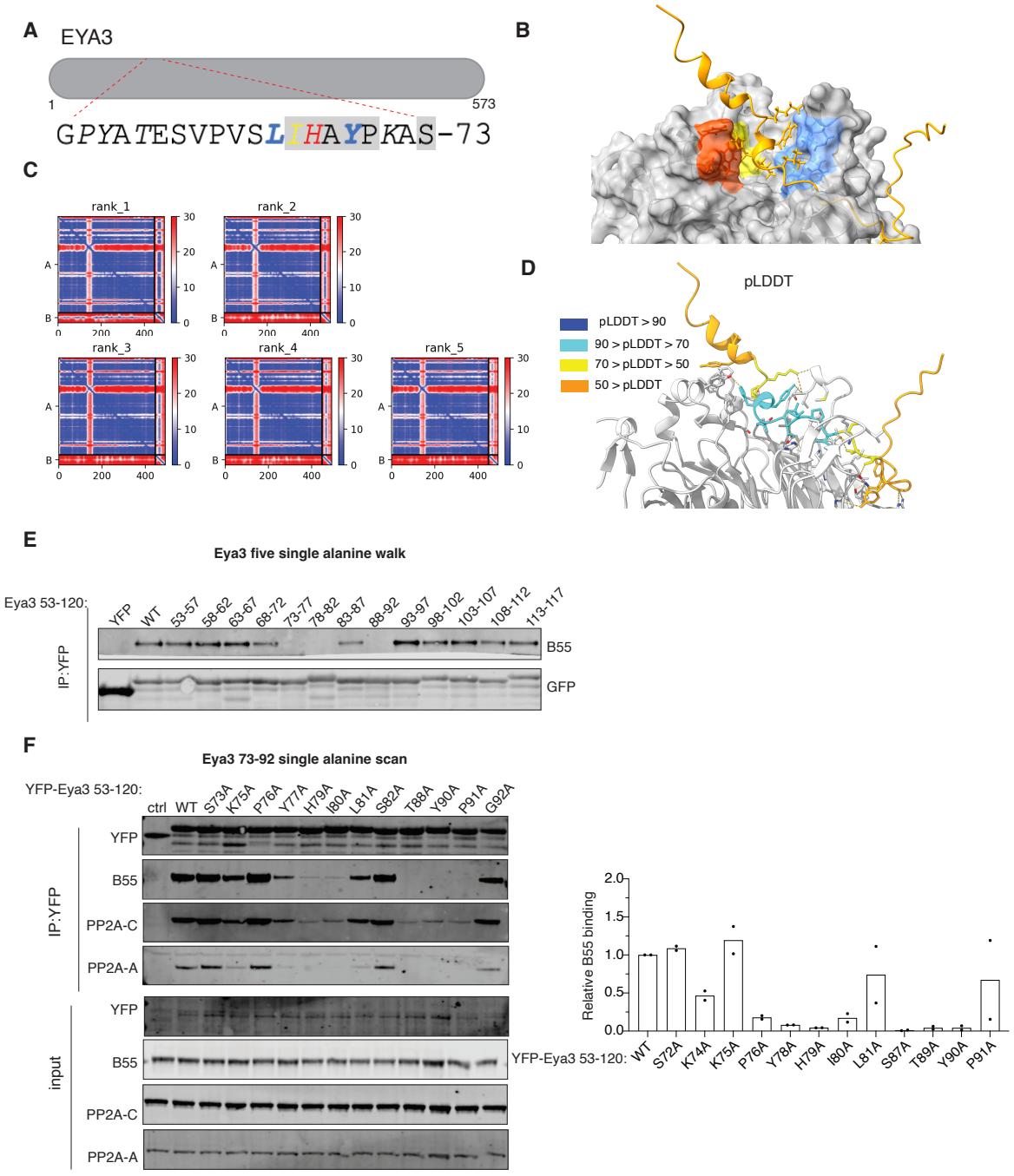

Supplemental Figure S7

A) Schematic of EYA3 and sequence binding PP2A-B55. **B**) AF model of EYA binding helix bound to B55. **C**) Prediction aligned error (PAE) score for the 5 models. **D**) pLDDT score mapped onto model. **E-F**) The indicated YFP tagged protein fragments were expressed in HeLa cells and following immunoprecipitation they were probed for binding to PP2A-B55 by western blot. In F) the quantification of two experiments is shown with binding normalized to wild type protein.

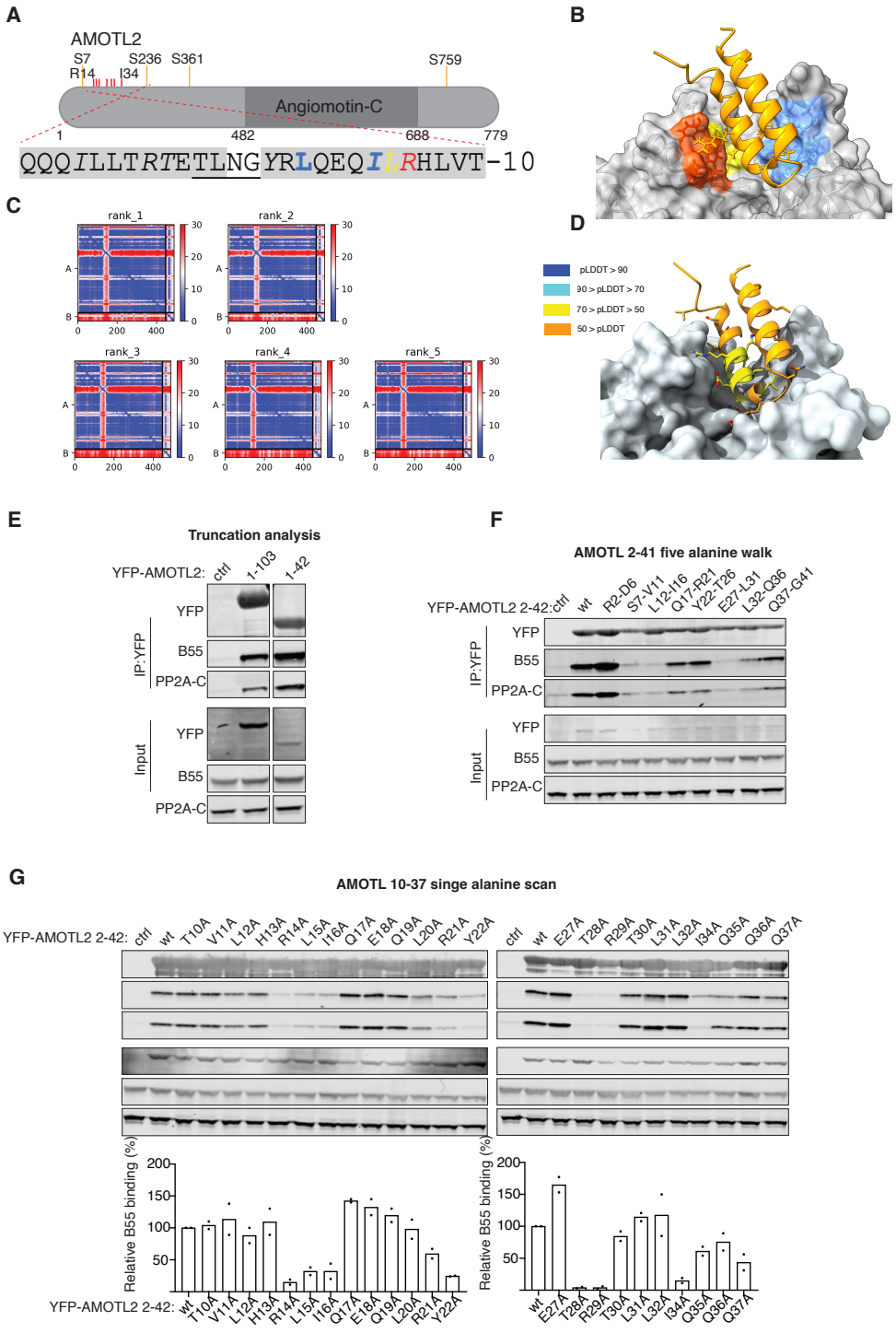

Supplemental Figure S8

A) Schematic of AMOTL2 and sequence binding PP2A-B55. Phosphorylation sites with higher occupancy in AMOTL2 T28A/R29A indicated **B**) AF model of AMOTL2 bound to B55. **C**) Prediction aligned error (PAE) score for the 5 models. **D**) pLDDT score mapped onto model. **E-I**) The indicated YFP tagged protein fragments were expressed in HeLa cells and following immunoprecipitation they were probed for binding to PP2A-B55 by western blot. In H) the quantification of two experiments is shown with binding normalized to wild type protein.

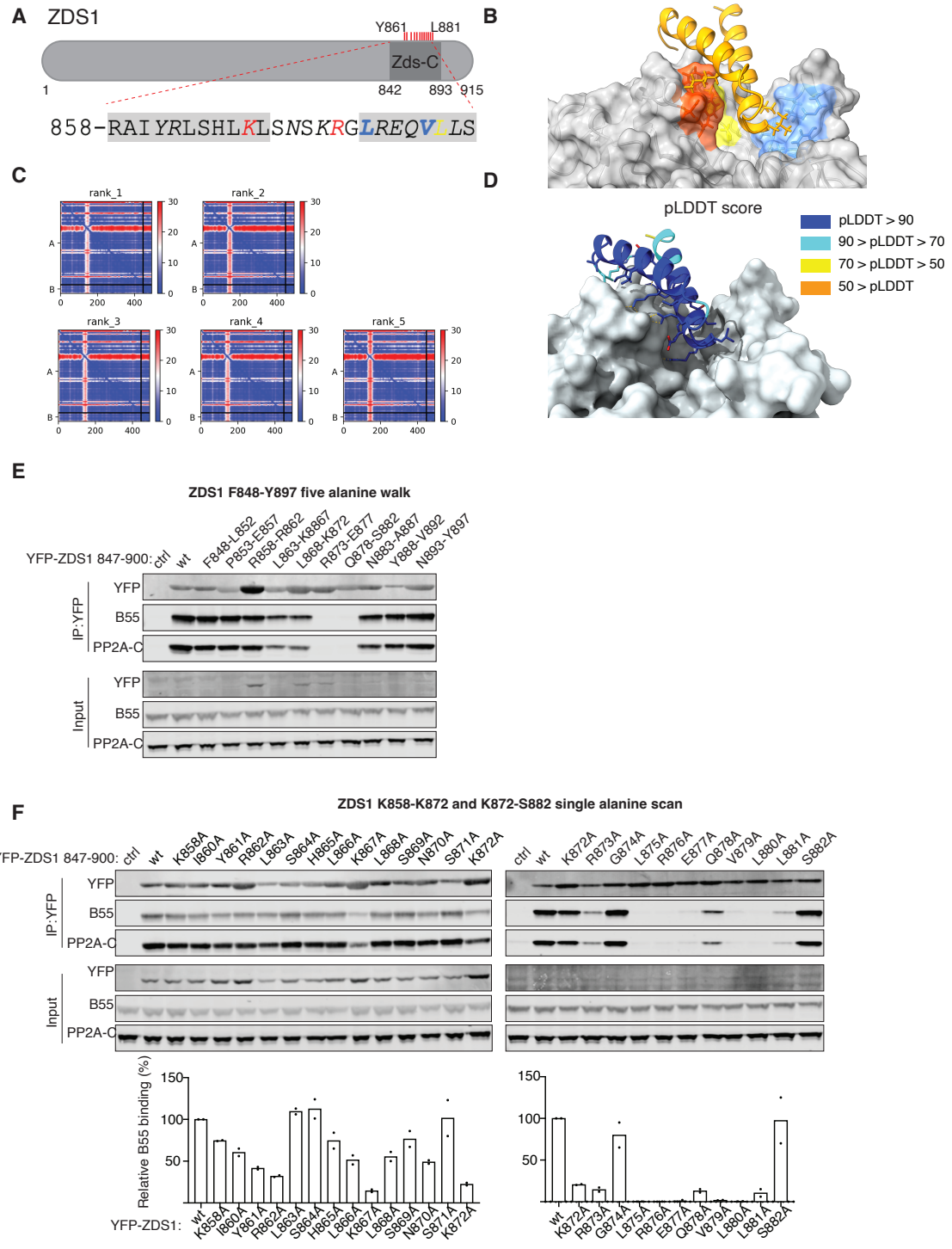

Supplemental Figure S9

A) Schematic of Zds1 and sequence binding PP2A-B55. **B**) AF model of Zds1 binding helixes bound to B55. **C**) Prediction aligned error (PAE) score for the 5 models. **D**) pLDDT score mapped onto model. **E-F**) The indicated YFP tagged protein fragments were expressed in HeLa cells and following immunoprecipitation they were probed for binding to PP2A-B55 by western blot. In F) the quantification of two experiments is shown with binding normalized to wild type protein.

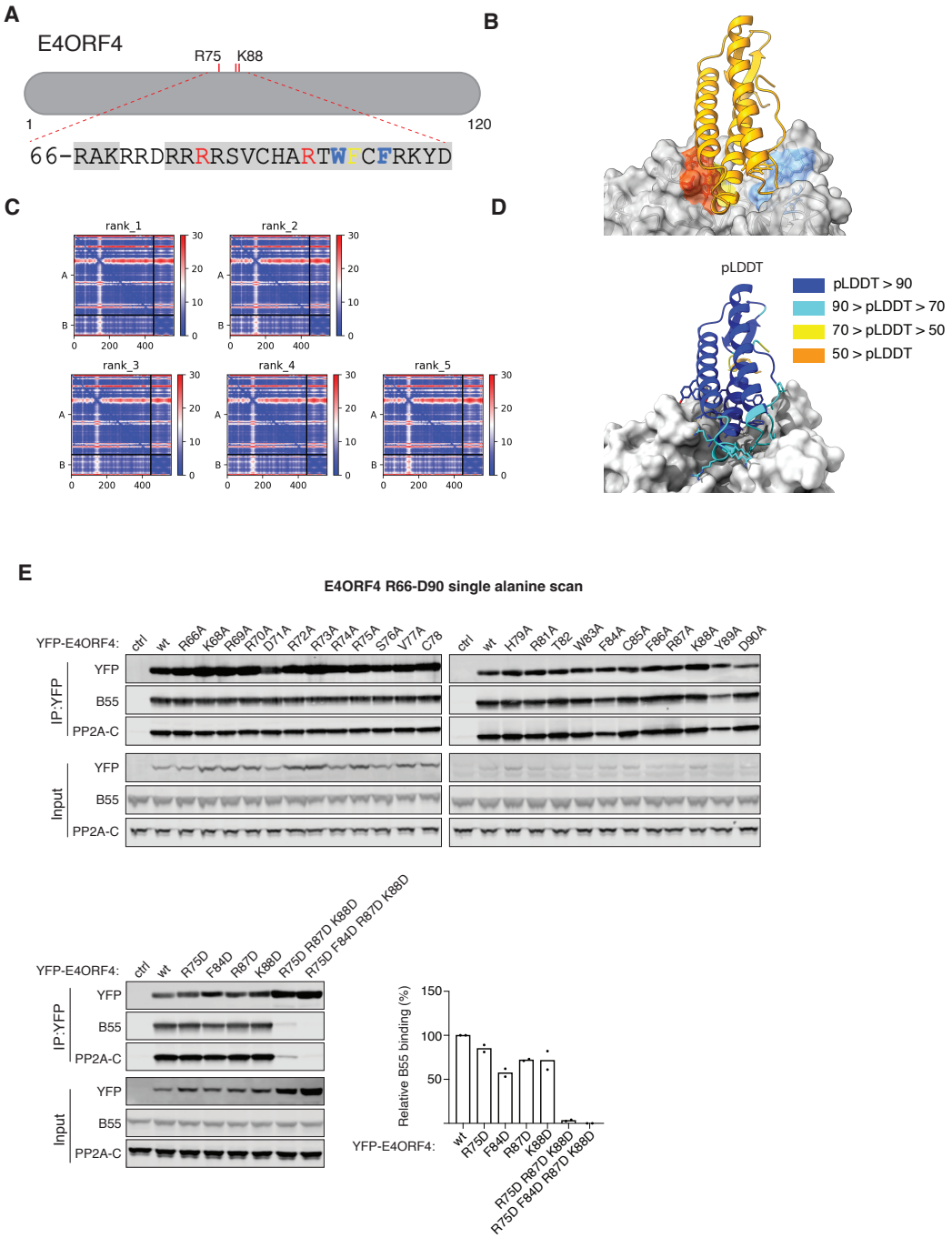

Supplemental Figure S10

A) Schematic of E4ORF4 and sequence binding PP2A-B55. **B**) AF model of E4ORF4 bound to B55. **C**) Prediction aligned error (PAE) score for the 5 models. **D**) pLDDT score mapped onto model. **E)** The indicated YFP tagged protein fragments were expressed in HeLa cells and following immunoprecipitation they were probed for binding to PP2A-B55 by western blot. **E)** Bottom panel the quantification of two experiments is shown with binding normalized to wild type protein.

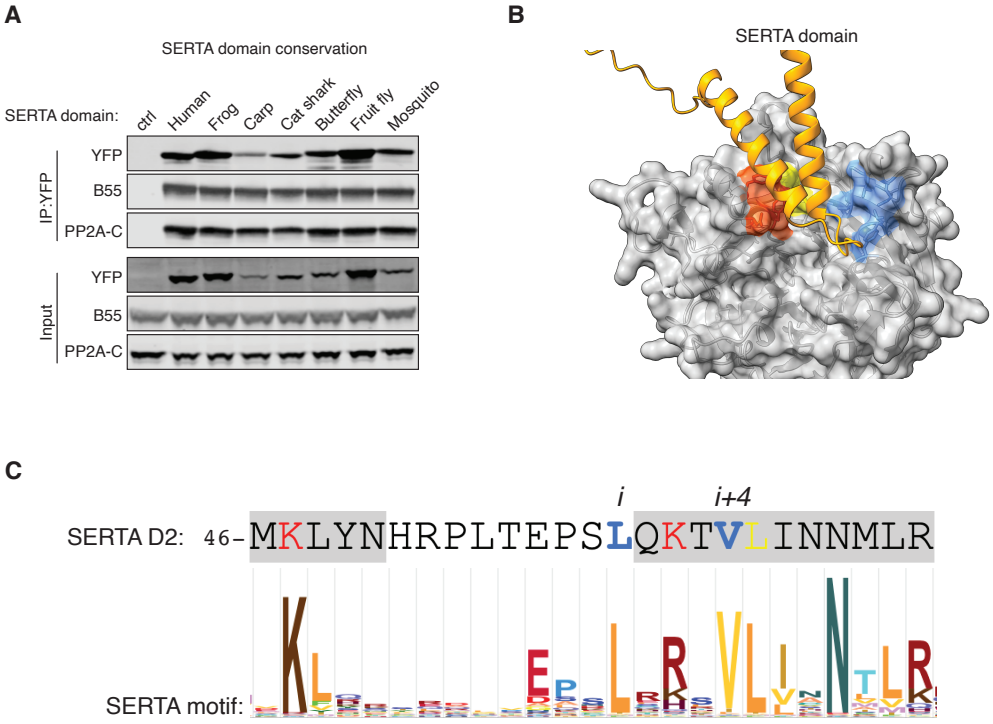

Supplemental Figure S11

A) YFP tagged SERTA domains from different species were expressed in HeLa cells and binding to PP2A-B55 determined by western-blot. **B**) AF model of the CDCA4 SERTA domain bound to B55. **C**) Signature of all SERTA domains in the pfam database showing conservation of key residues (data from pfam 06031)

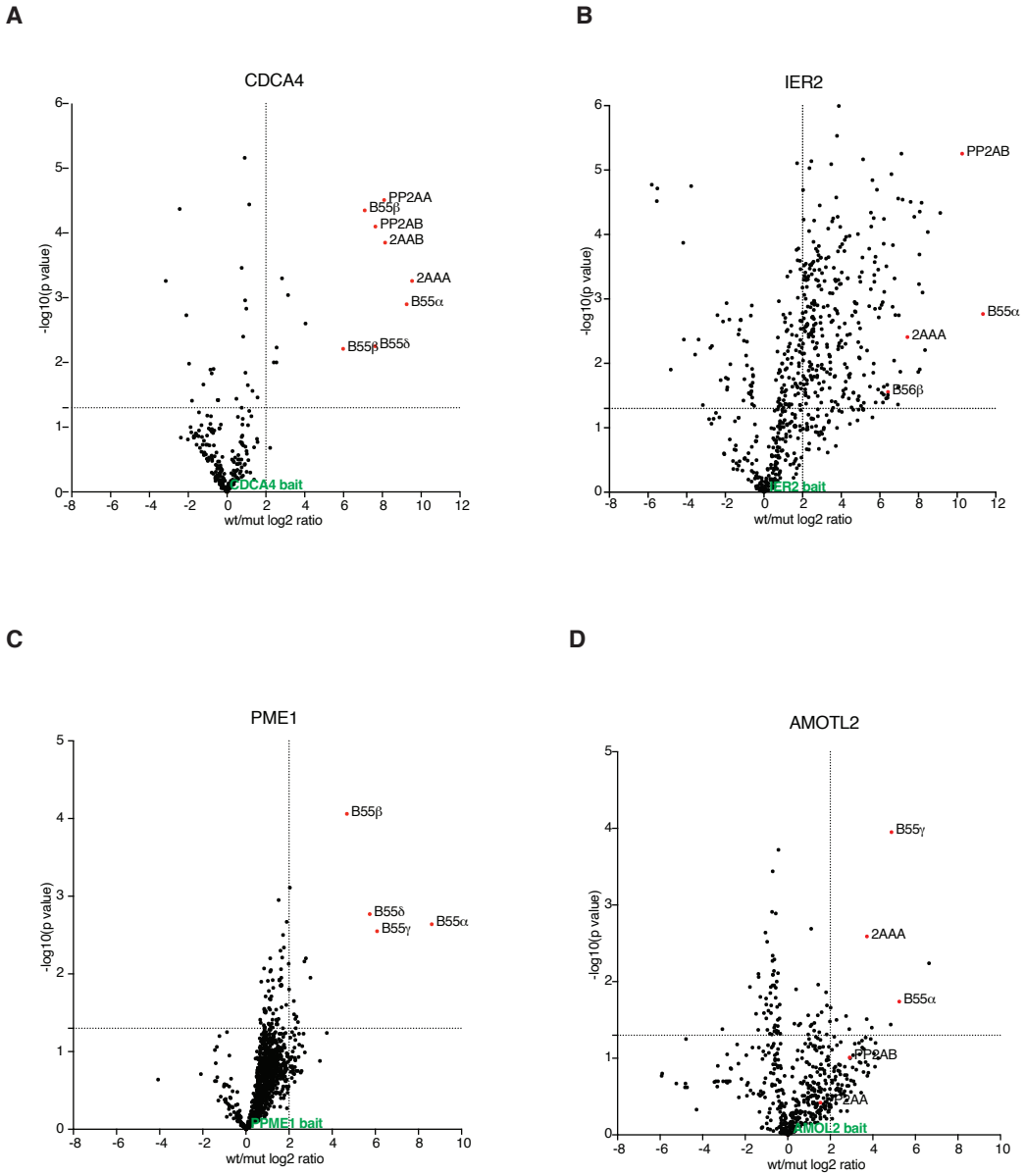

Supplemental Figure S12

A-D) Volcano plots of mass spectrometry analysis of immunopurifications (n=4) of the indicated proteins comparing wild type to B55 mutant. PP2AA/B: catalytic subunit, 2AAA: scaffold subunit.

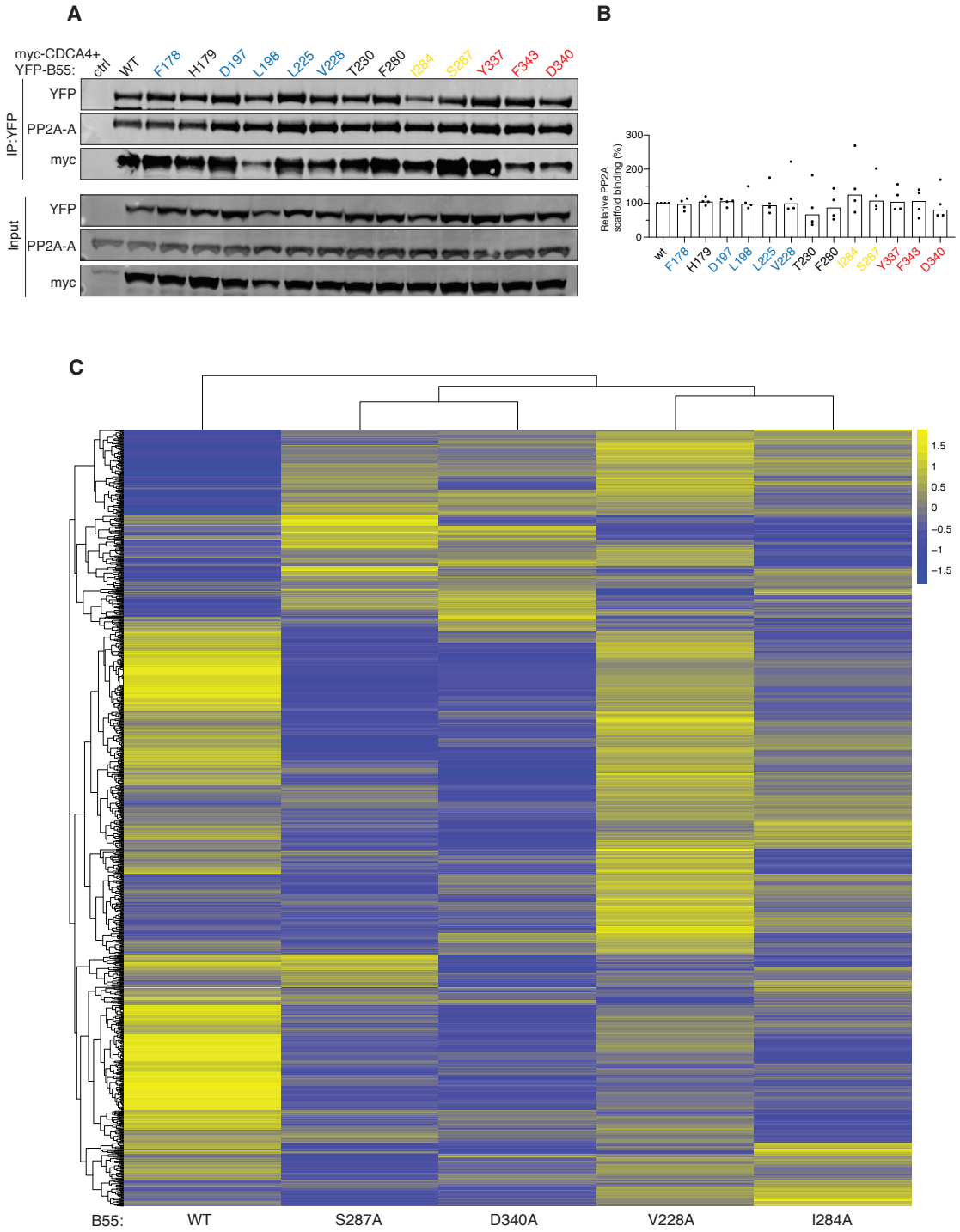

Supplemental Figure S13

A) Immunoprecipitation of indicated YFP-B55 tagged mutants and binding to myc-CDCA4 determined by western blot **B)** Quantification to relative binding of PP2A scaffold to B55 mutants; median shown, n=4. **C**) HEAT map relating to Figure 2 showing all proteins identified by mass spectrometry in the different B55 variants. Scale bar is log2 and n=4.

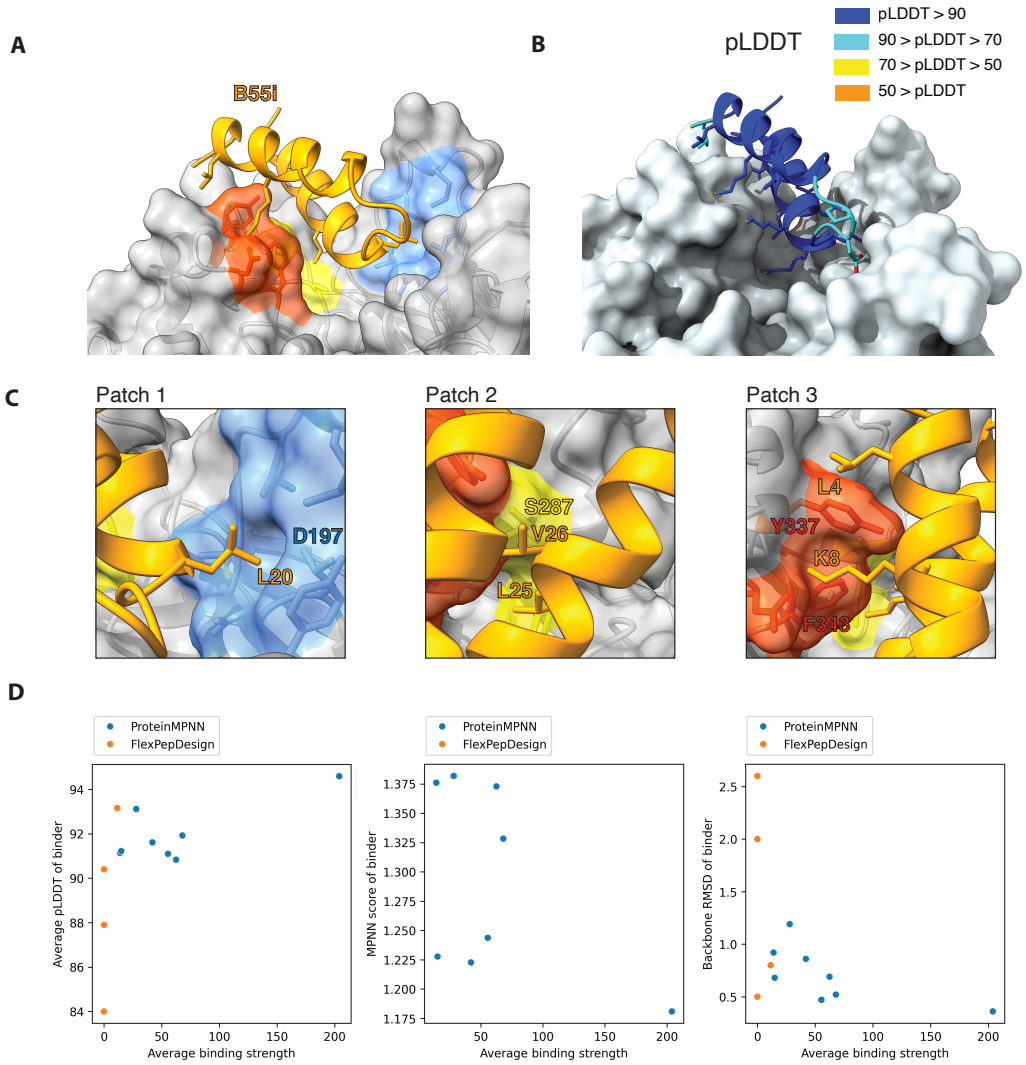

Supplemental Figure S14

A-B) AF model of B55i bound to B55 and pLDDT score. **C**) Zoom in on interactions of B55i with the different patches. **D**) Plots of design scores and binding strength based on immunopurifications from HeLa cells of YFP tagged de novo B55 binders.

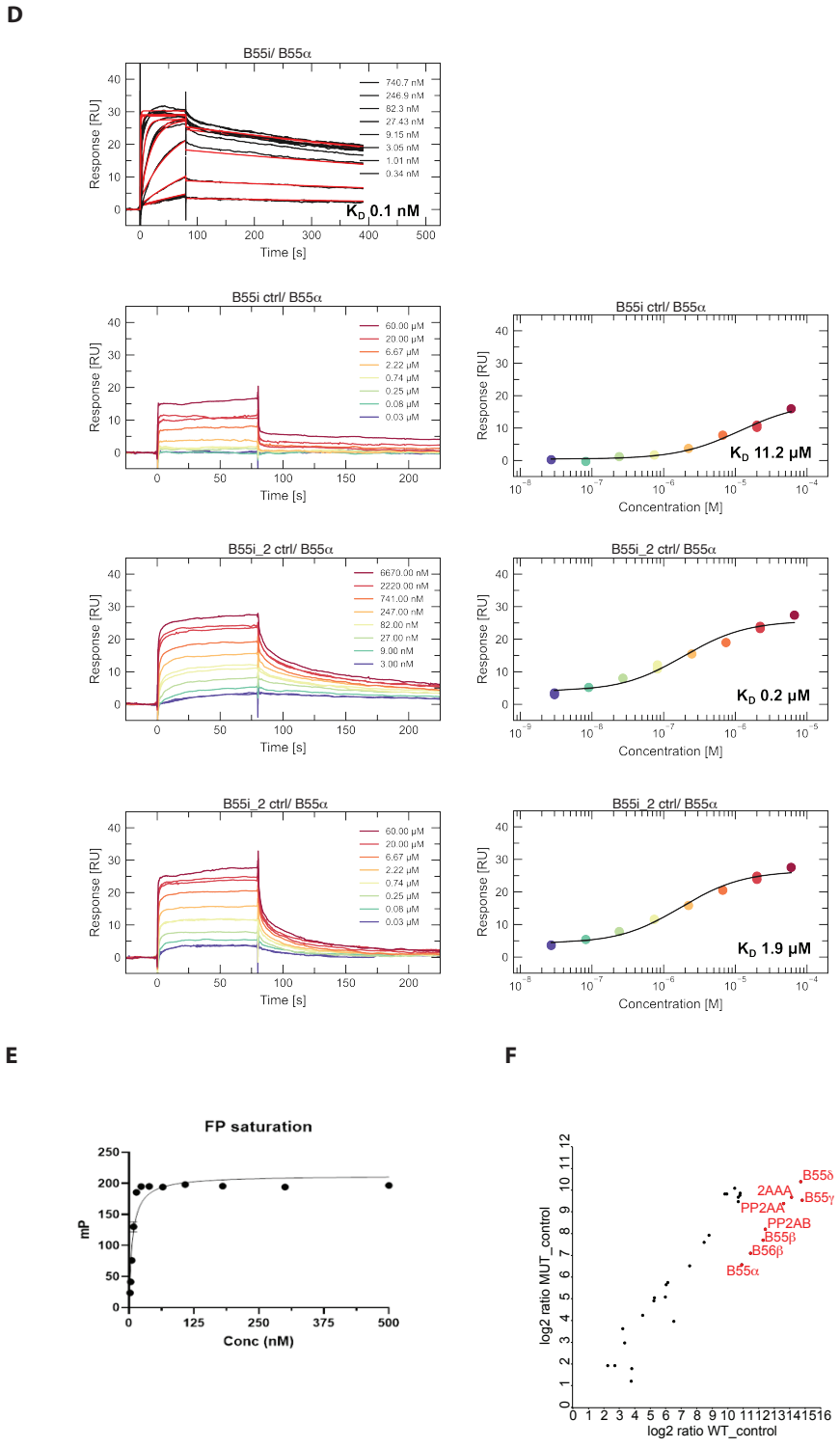

Supplemental Figure S14-continued

D) SPR data for B55i-1 and B55i-2 peptides binding to B55. **E**) FP measurements for B55i (n=3). **F**) Mass spectrometry analysis of B55i and B55i CTRL based on n=4.

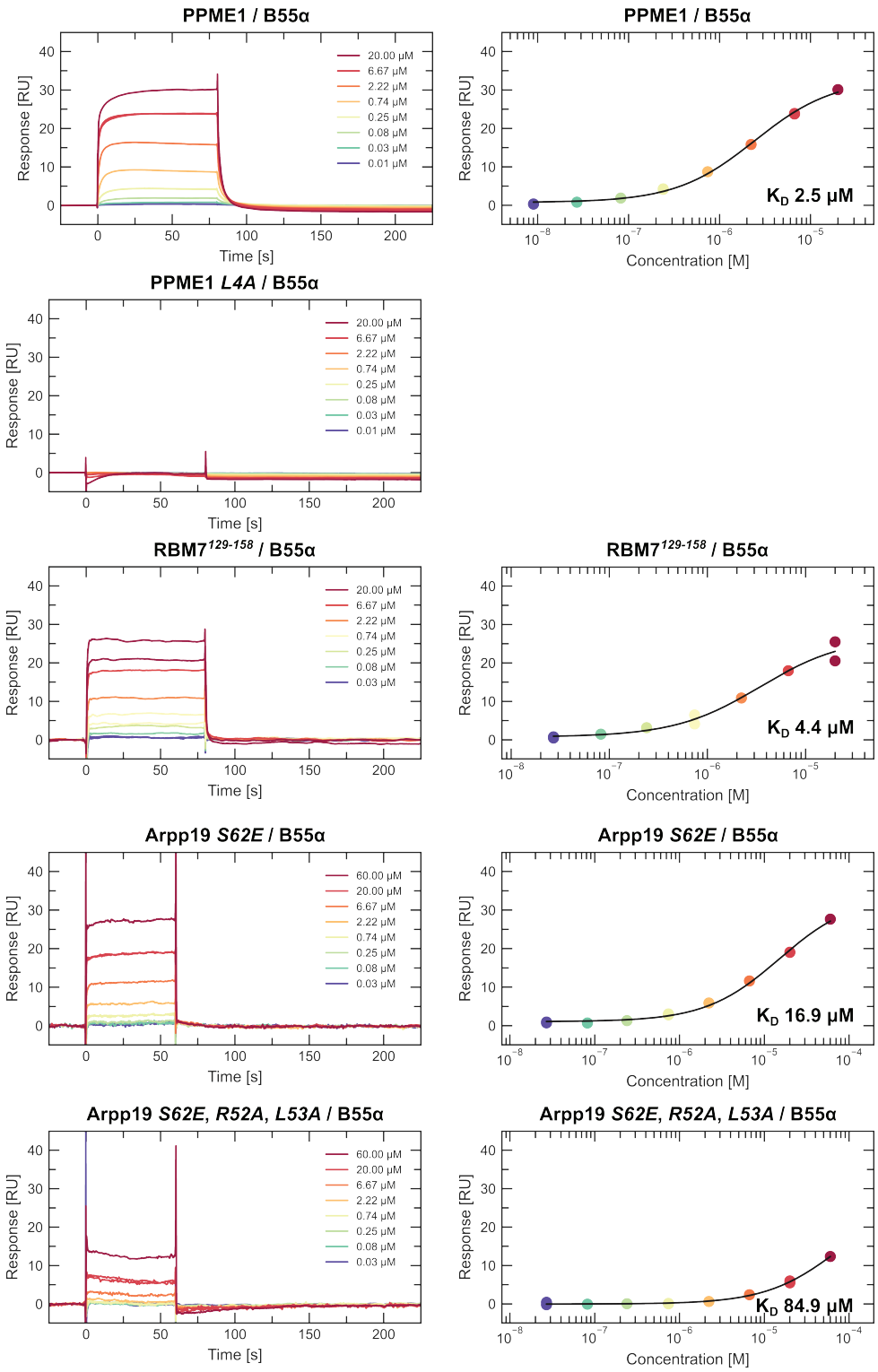

Supplemental Figure S15

SPR data for the indicated proteins binding to B55.

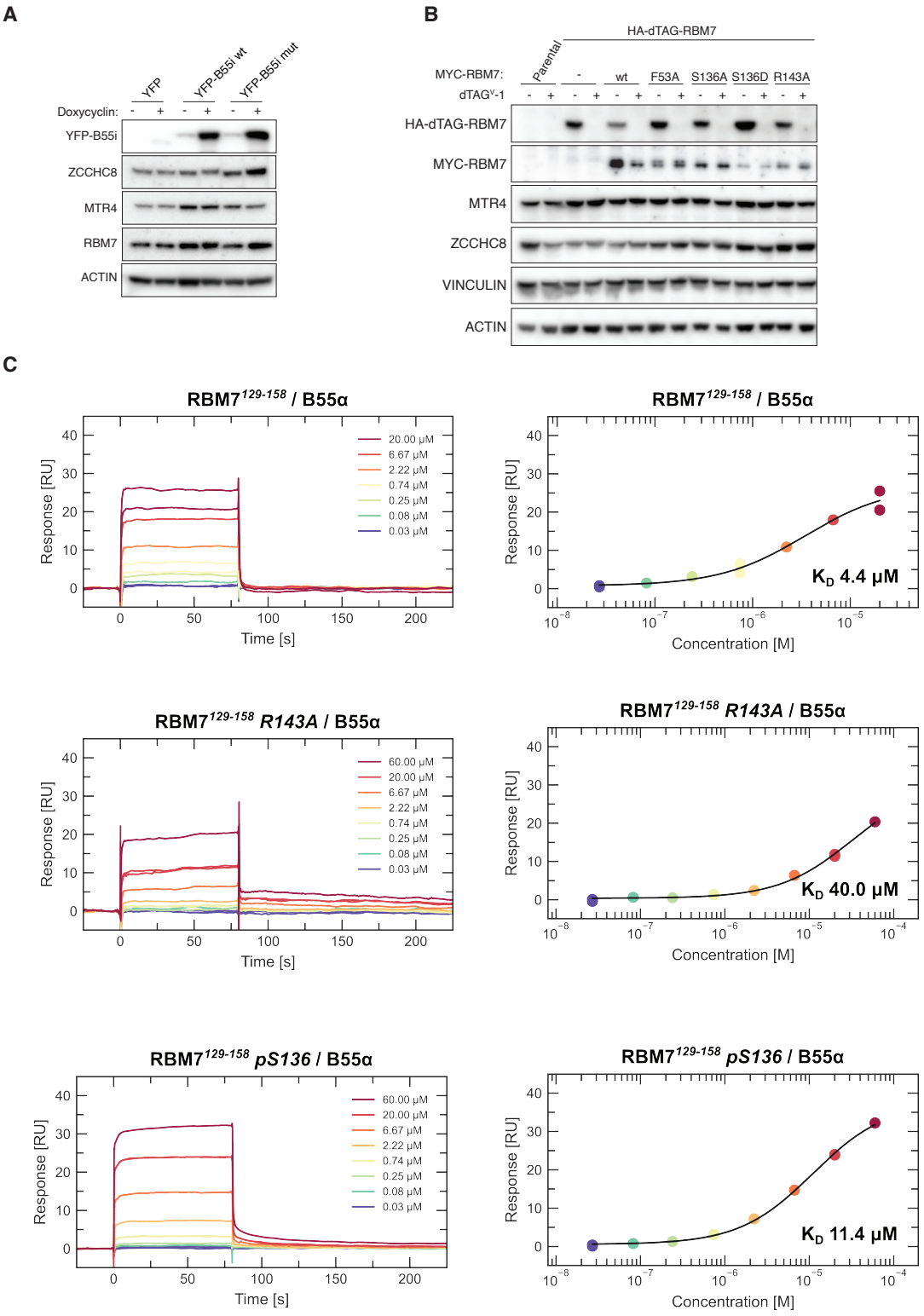

Supplemental Figure S16

A) Western blots of B55i expression from inducible HeLa cells. **B**) Removal of HA-dTAG-RBM7 with dTAG-1 and complementation with myc-RBM7 variants. **C**) SPR data for the indicated RBM7 peptides binding to B55.